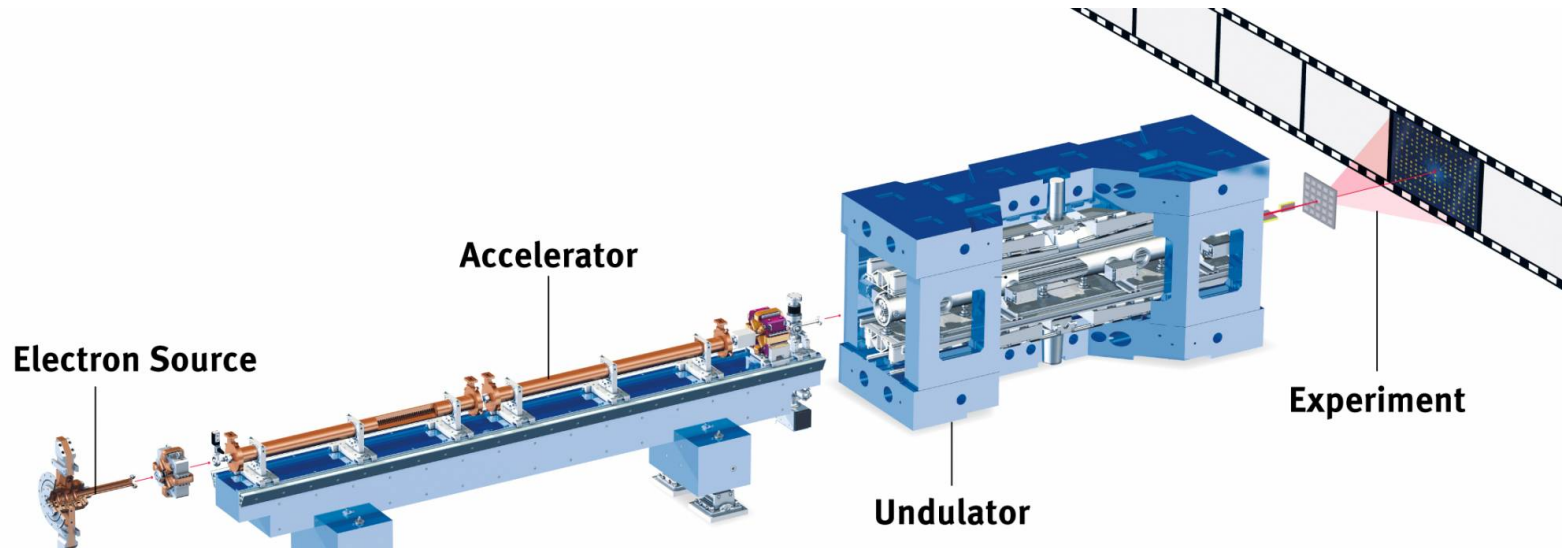


# Wire Scanner on a Chip

*S. Borrelli, M. Bednarzik, C. David, E. Ferrari, A. Gobbo, V. A. Guzenko, N. Hiller,  
R. Ischebeck, G.L. Orlandi, C. Ozkan-Loch, B. Rippstein and V. Schlott.*

# Free Electron Laser



In a FEL machine it is important to preserve the e-beam **normalized emittance** in order to produce laser pulses of the desired wavelength.

## SwissFEL Nominal e-Beam Parameters

E	5.8 GeV
Q	200-10 (pC)
$\epsilon_N$	0.4-0.2 (mm mrad)
$\sigma_{\min}$ (@10 pC)	8 $\mu\text{m}$ (rms)



High resolution emittance measurements necessary.

# The ACHIP Project

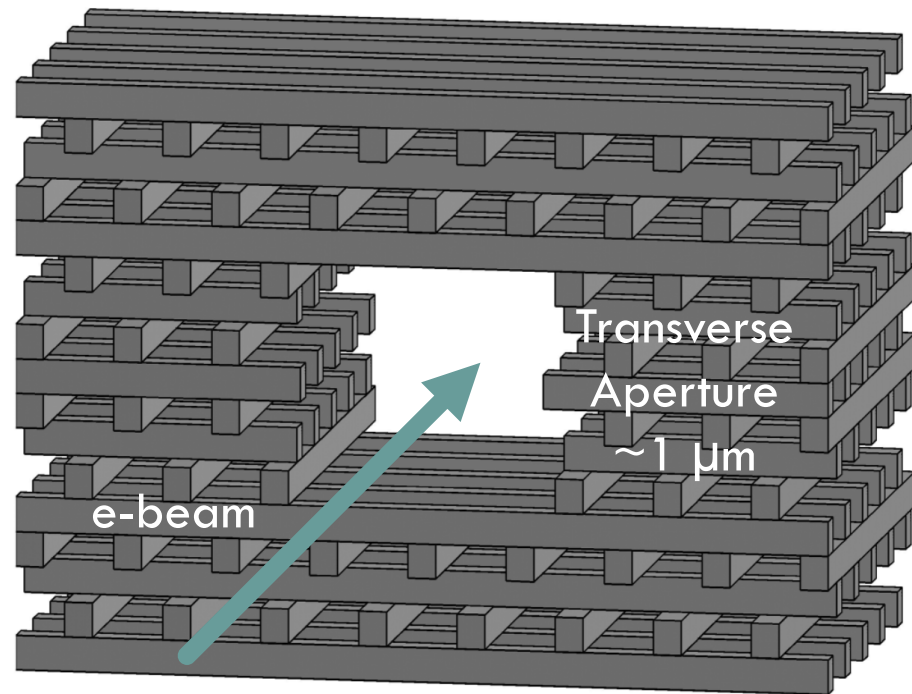
GORDON AND BETTY  
**MOORE**  
FOUNDATION



Compact electron accelerator in which the accelerator structure is a dielectric microstructure excited by femtosecond laser pulses.

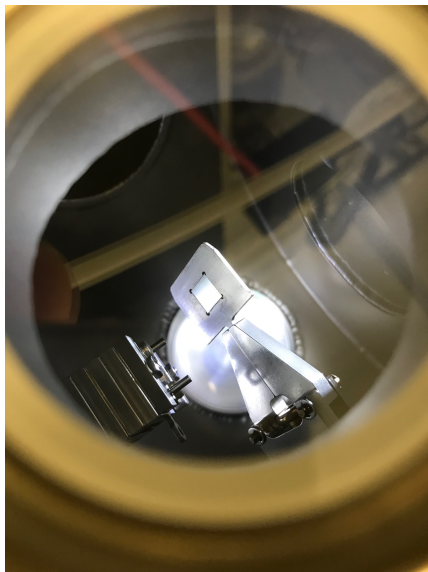
(Dielectric Laser Accelerator)

Sub-micrometric beam size and low emittance is necessary.



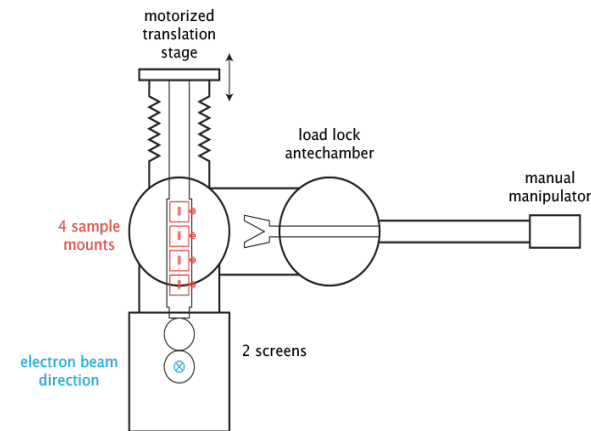
# The ACHIP Project at SwissFEL

Proof-of-principle demonstration of the acceleration of a highly relativistic beam at SwissFEL.



## SwissFEL Injector ACHIP chamber

Load-lock chamber to **install four** different **samples** without breaking beamline vacuum.



## SwissFEL ATHOS ACHIP chamber

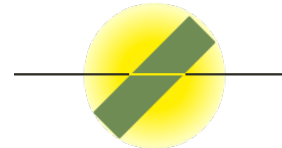
A second ACHIP chamber will be installed in the **SwissFEL ATHOS line**.  
Expected spot size  $< 1\mu\text{m}$

# Beam Transverse Profile Monitors

## 2-D Monitors

### Scintillating crystals

YAG:Ce Screen

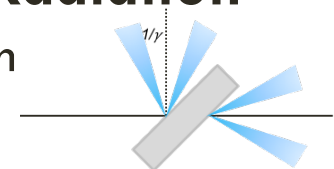


- High dynamic range but not linear
- Possible saturation
- Resolution is **8  $\mu\text{m}$**  (rms) (SwissFEL )

Ischebeck, R., et al. "Transverse profile imager for ultrabright electron beams." *PRST-AB* 18.8 (2015): 082802.

### Optical Transition Radiation

OTR Screen



- Linear
- Coherent OTR emission from compressed bunch

Akre, R., et al. "Commissioning the linac coherent light source injector." *PRST-AB* 11.3 (2008): 030703.

## Synchrotron Radiation Monitor

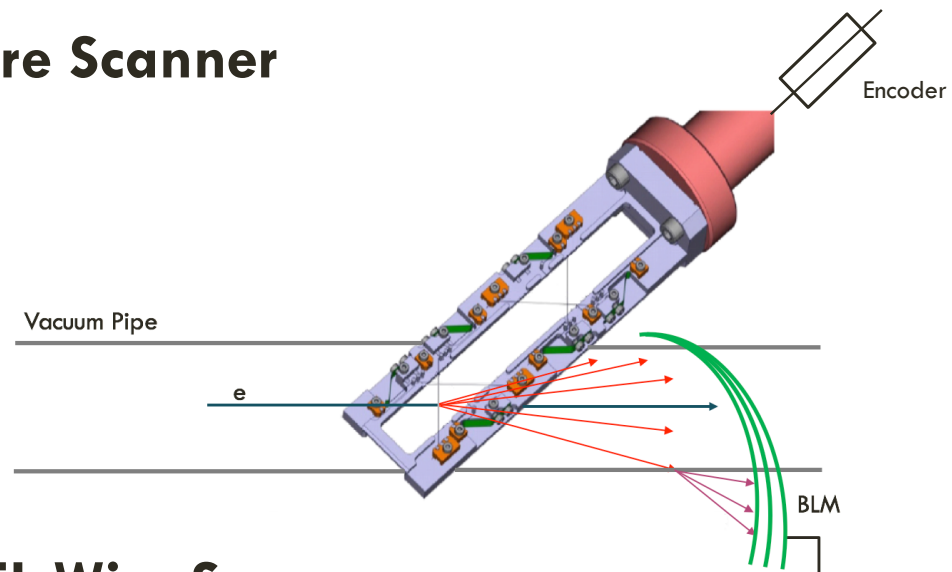
- Linear in case of no coherent radiation emission
- Not affected by saturation
- Resolution **6  $\mu\text{m}$**  (rms) SLS  
**~50  $\mu\text{m}$**  SwissFEL

Andersson, Å., et al. "Determination of a small vertical electron beam profile and emittance at the Swiss Light Source." *Nuc.Instr. and Methods in Physics Research Section A: Accelerators, Spectrometers, Detectors and Associated Equipment* 591.3 (2008): 437-446.

# Beam Transverse Profile Monitors

- 1-D monitor
- Multi shot measurement
- Resolution limited by
  - Wire diameter
  - Wire vibration
  - Beam jitter
  - Encoder resolution

## Wire Scanner



## SwissFEL Wire Scanner

- Geometrical resolution (5  $\mu\text{m}$  W wires) 1.25  $\mu\text{m}$
- Wire vibration within the geometrical resolution limit
- Encoder resolution 0.1  $\mu\text{m}$

Orlandi, G. L., et al. "Design and experimental tests of free electron laser wire scanners." *PRA*, 19.9 (2016): 092802.

Wire scanner commissioning >>> WEPCC16 Poster by G.L.Orlandi

Reduce wire diameter  
to improve resolution



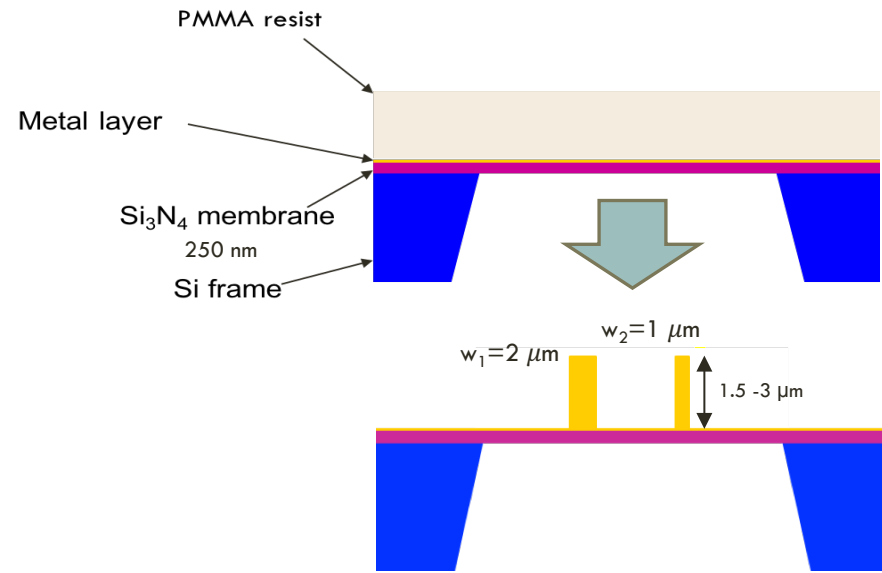
IDEA

Use the nanofabrication of sub-micrometer metallic stripes on a membrane via e-beam lithography.

# Sub-micrometer Resolution Wire Scanner

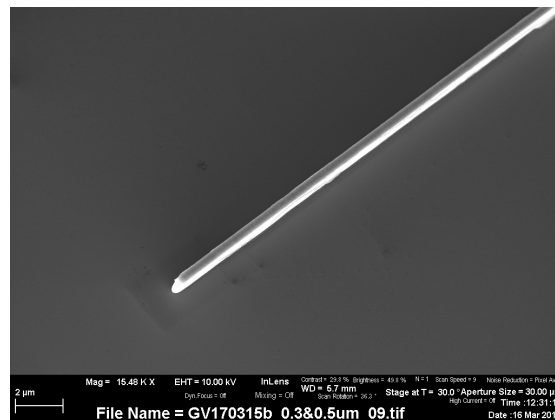
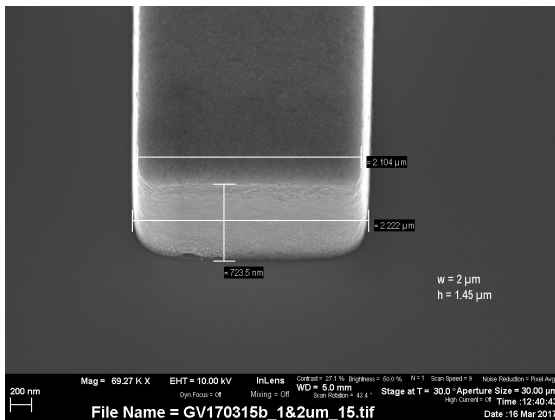
## Fabrication Technique

- Electron Beam Lithography on the Resist
- Resist development
- Top Cr layer removal
- Electroplating of two Au wires of different widths ( $w_1, w_2$ )
- Resist removal

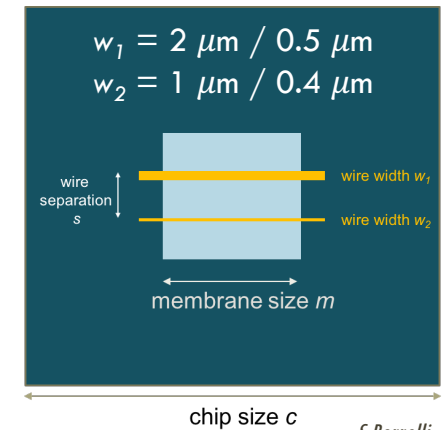


## Scanning Electron Microscope characterization

Vitaliy Guzenko

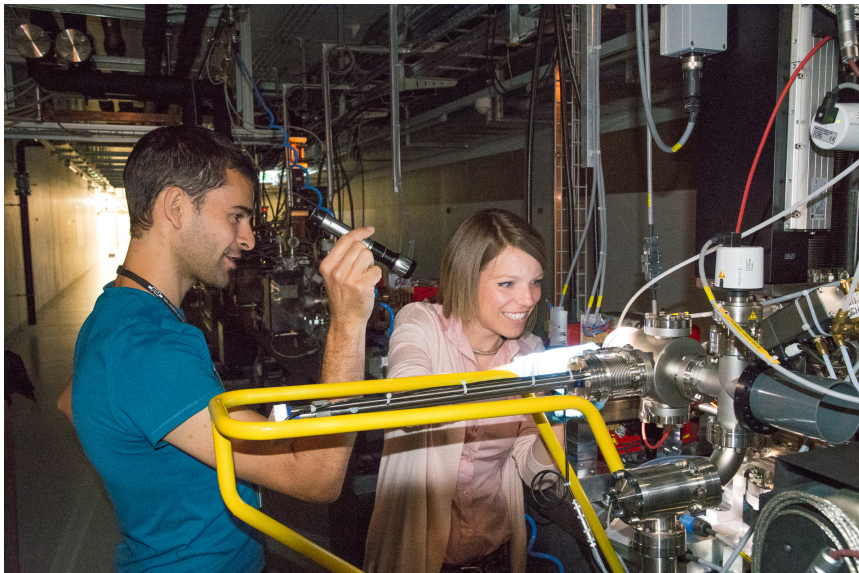
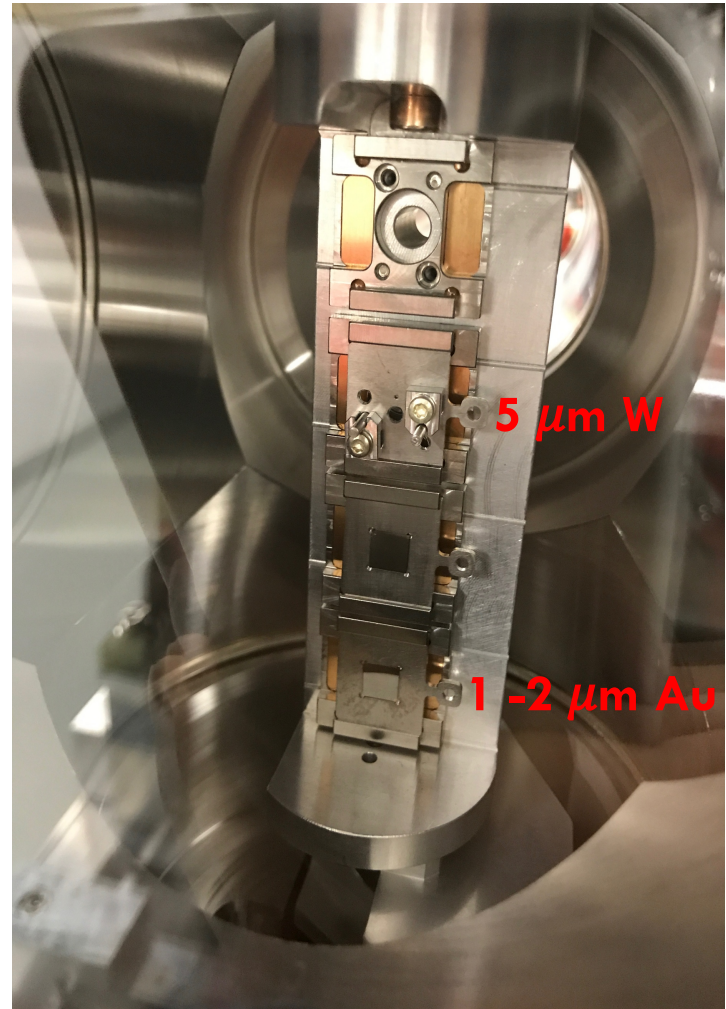
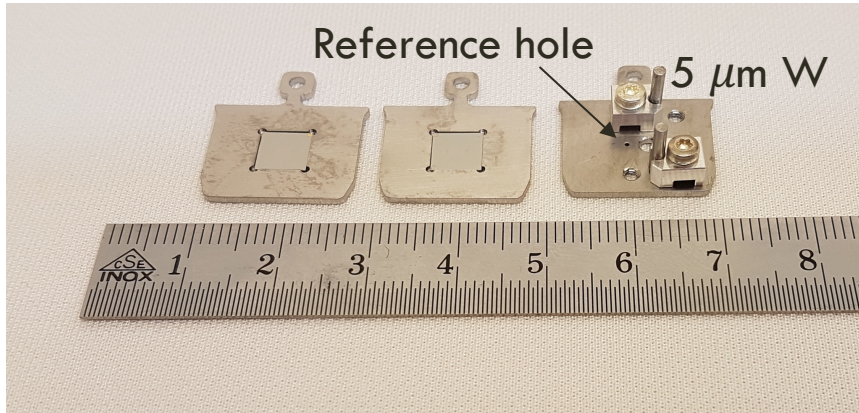


## Prototype Sketch



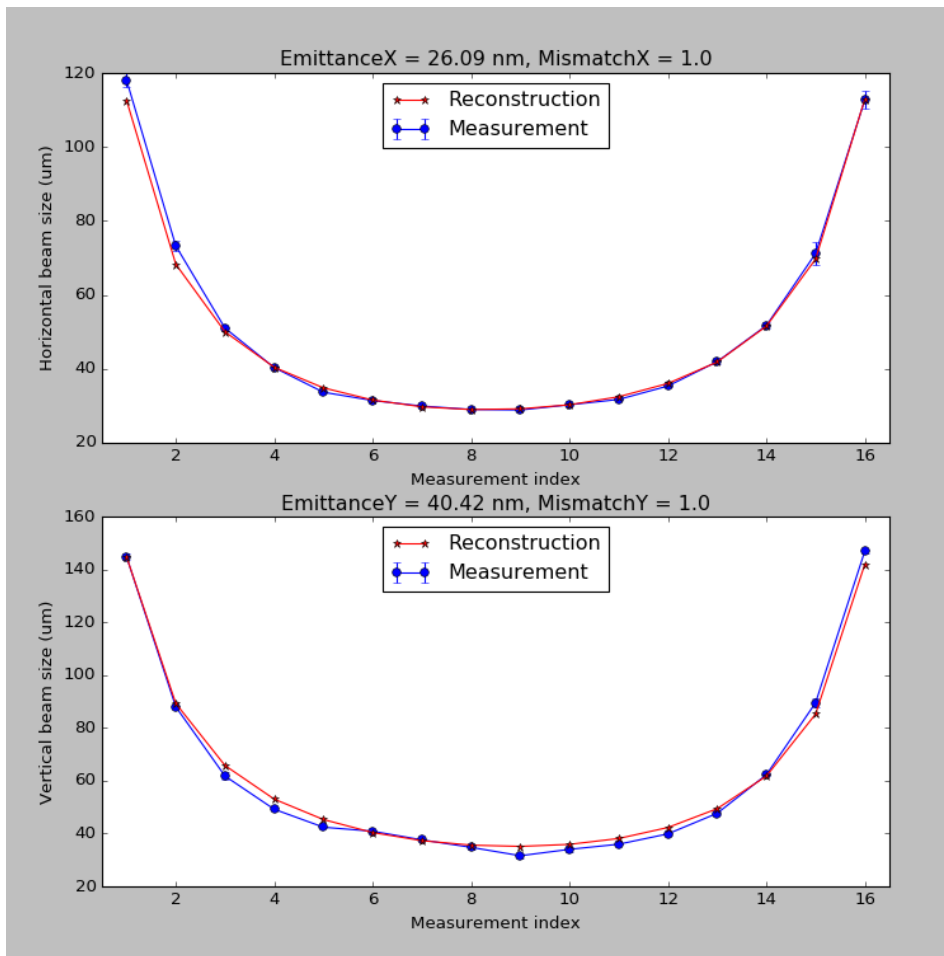
# Sub-micrometer Resolution Wire Scanner

## Prototype Installation



# First Experimental Results

## Optics Settings



## Beam Parameters

Energy	=	330 MeV
Charge	=	200 fC
$\epsilon_x, \epsilon_y$	=	30, 40 nm

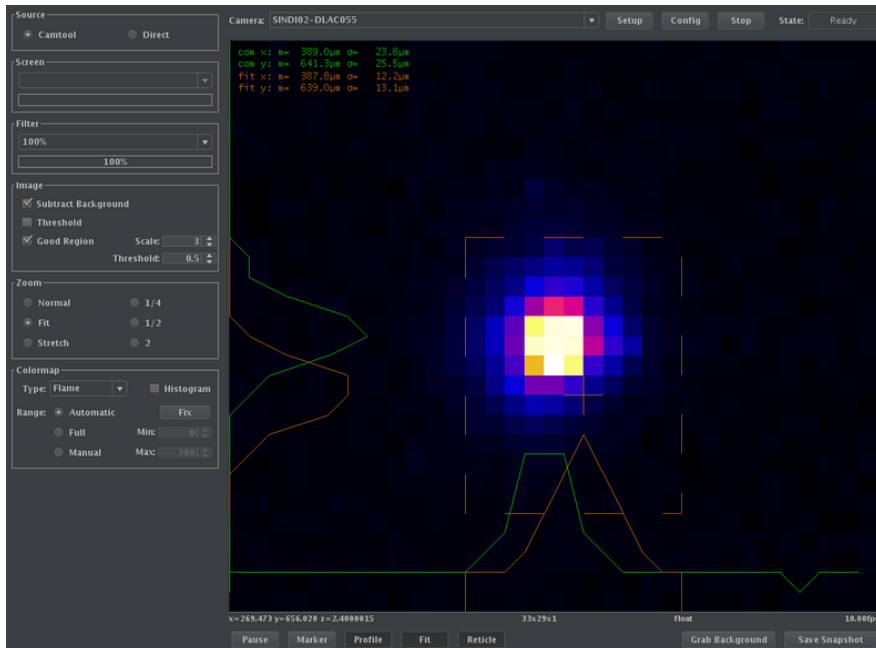
## Optics

## Expected Beam Size

$$\begin{aligned}\sigma_x &= 2.7 \mu\text{m} \\ \sigma_y &= 3.2 \mu\text{m}\end{aligned}$$

# First Experimental Results

## Screen Beam Profile Measurement

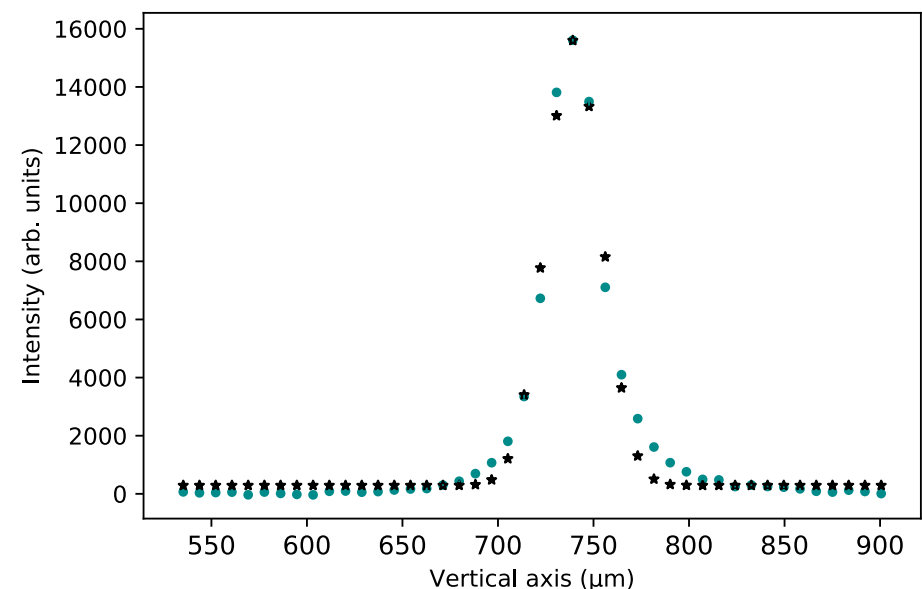


\*YAG:Ce screen beam size measurement is limited by a resolution of  $\sim 14 \mu\text{m}$ .

### Gauss Fit

$$\bar{\sigma}_y = 14.4 (\mu\text{m})^*$$

Mean over 100 images



# First Experimental Results

## 5 $\mu\text{m}$ W WSC Beam Profile Measurement

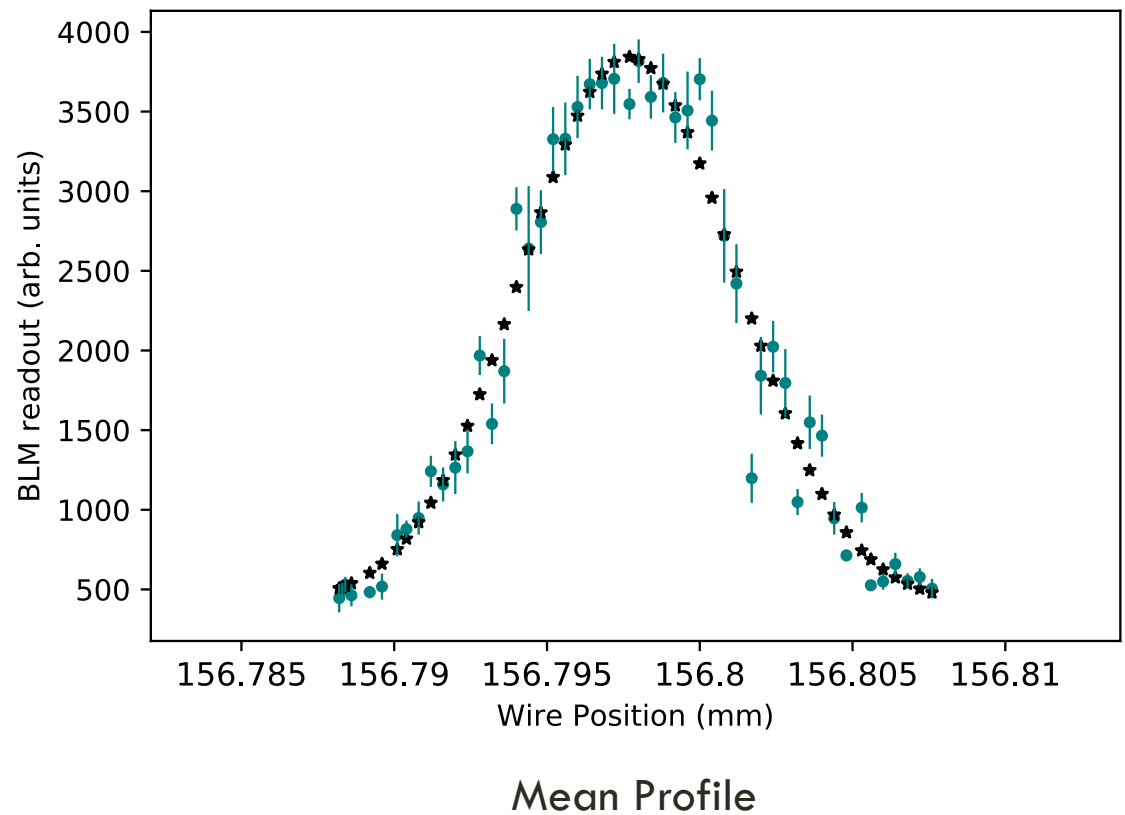
**Gauss Fit**

$$\bar{\sigma}_y = 3.52 \pm 0.02 \text{ } (\mu\text{m})$$

Mean over 10 scan cycles

**Signal to noise  
ratio**

$$\text{SNR} = 13$$



# First Experimental Results

## 2 $\mu\text{m}$ Au WSC Beam Profile Measurement

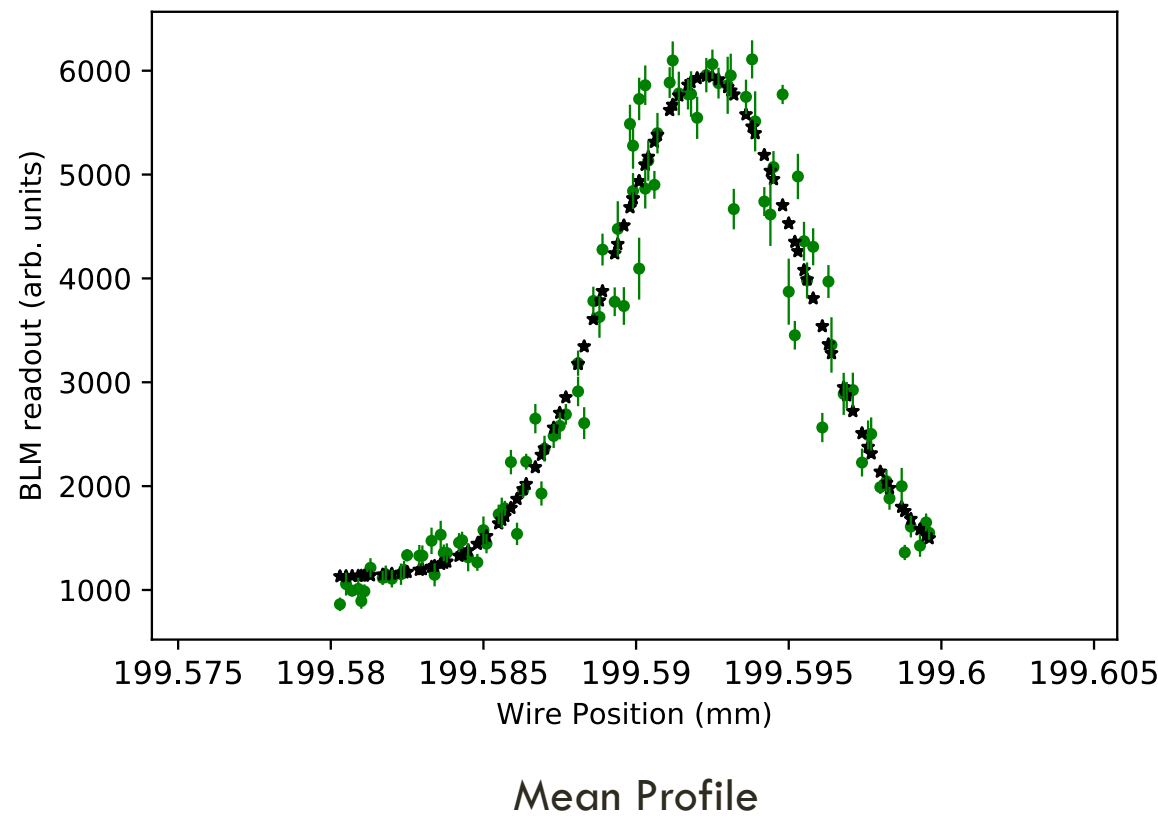
**Gauss Fit**

$$\bar{\sigma}_y = 3.21 \pm 0.04 (\mu\text{m})$$

Mean over 10 scan cycles

**Signal to noise  
ratio**

$$\text{SNR} = 7$$



# First Experimental Results

## 1 $\mu\text{m}$ Au WSC Beam Profile Measurement

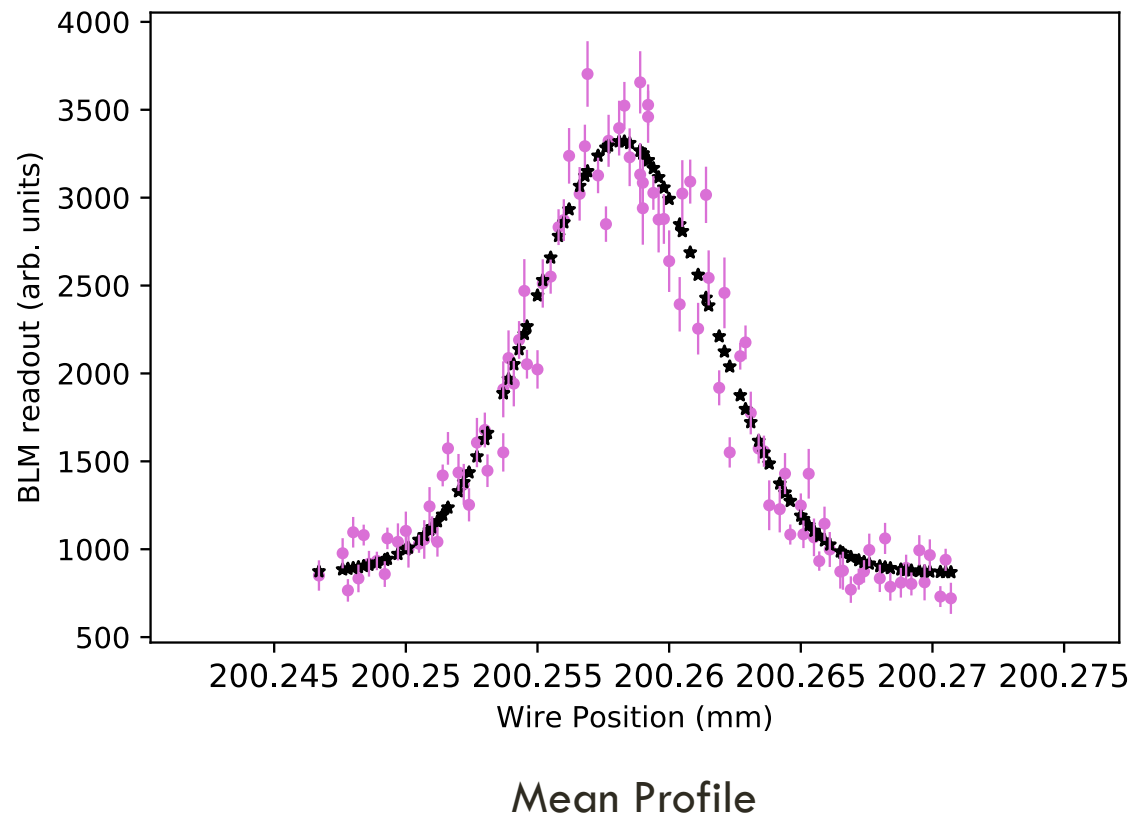
**Gauss Fit**

$$\bar{\sigma}_y = 3.37 \pm 0.06 (\mu\text{m})$$

Mean over 10 scan cycles

**Signal to noise  
ratio**

$$\text{SNR} = 5$$



# Background From The Membrane

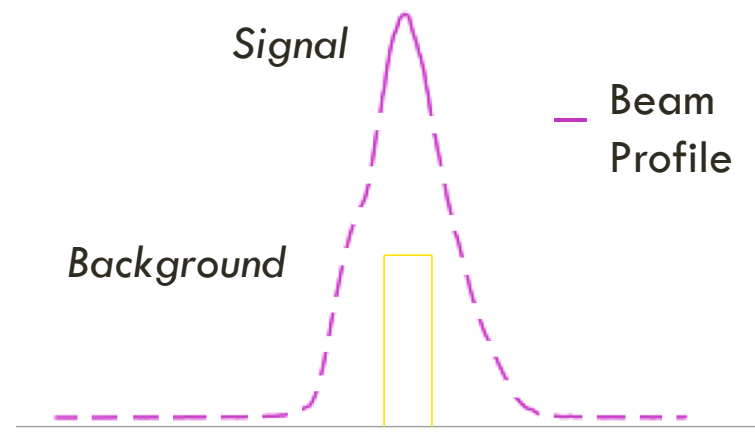
Measured Values	5 μm W	2 μm Au	1 μm Au
SNR	13	7	5

Signal to Noise ratio degraded by the membrane.

## Background to signal ratio

$$\frac{\Delta E|_{rad}^{Si_3N_4}}{\Delta E|_{rad}^{Si_3N_4+Au}} = 18$$

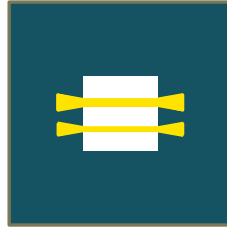
From the radiative energy loss in the membrane + wire thickness and in the membrane thickness.



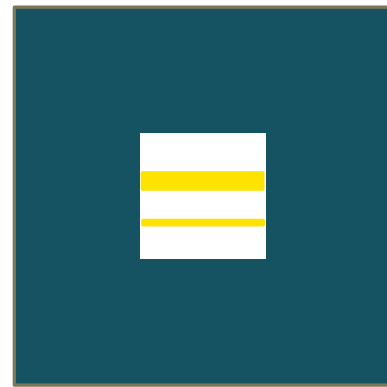
Only a small fraction of the beam cross the membrane and the wire producing the signal of interest.

# Outlook

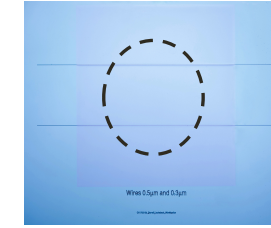
## Signal to Noise Ratio Improvement



Reshape the wires



Remove the membrane



Remove a central hole  
in the membrane

## Measure Resolution Limit

Measure a sub-micrometric beam profile focusing the beam in the ATHOS ACHIP chamber via in vacuum quadrupoles.

# Thanks so much!

*Gian Luca Orlandi*

*Rasmus Ischebeck*

*Vitaliy Guzenko*

*Cigdem Ozkan*

*Eugenio Ferrari*

*Volker Schlott*

*Nicole Hiller*

*Eduard Prat*

*Josh McNeur*

*Simona Bettoni*

*PSI Vacuum Group*

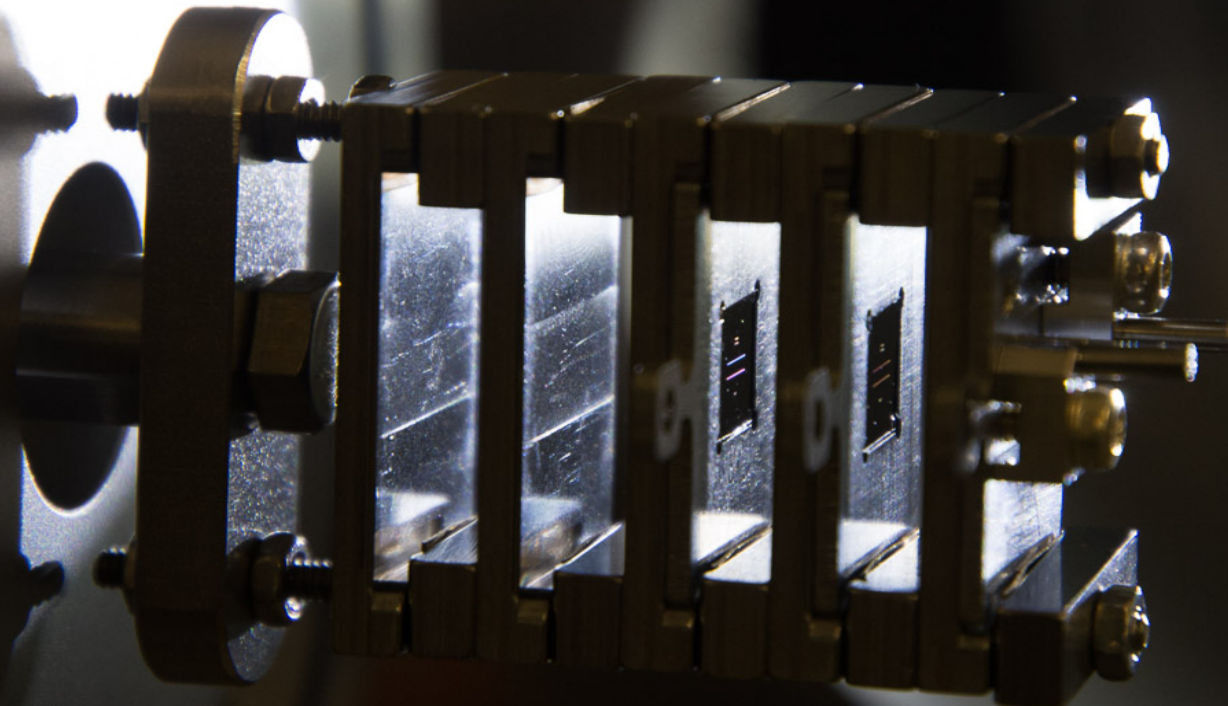
*Christian David*

*Martin Bednazik*

*Beat Rippstein*

*Alexandre Gobbo*

*Arturo Daniel Alarcon*



# Wire Scanner on a Chip

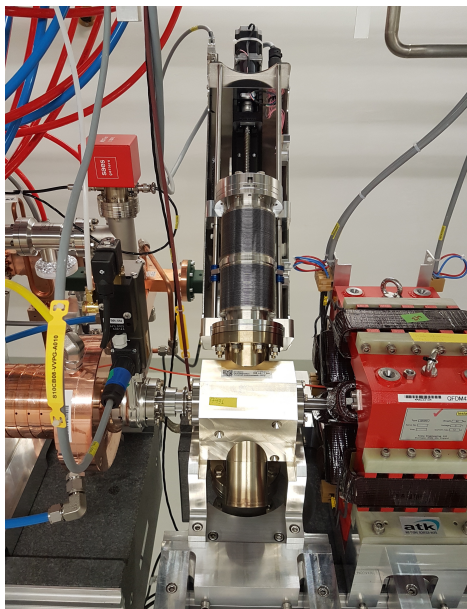
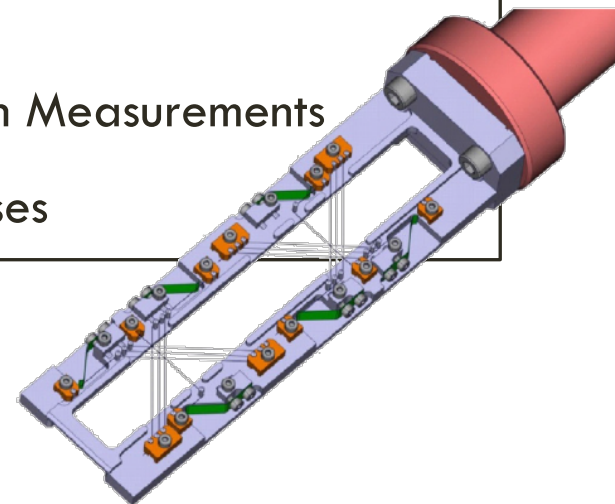
*S. Borrelli, M. Bednarzik, C. David, E. Ferrari, A. Gobbo, V. A. Guzenko, N. Hiller,  
R. Ischebeck, G.L. Orlandi, C. Ozkan-Loch, B. Rippstein and V. Schlott.*

# BACKUP SLIDES

# SwissFEL WIRE SCANNER

SwissFEL Wire Scanners (WSCs) consist of a wire fork equipped with two couples of wires:

- 5  $\mu\text{m}$  W wires High Resolution Measurements
  - 12.5  $\mu\text{m}$  Al(99):Si(1) wires Low Beam Losses



Fork inserted in the vacuum by means of an Ultra-High Vacuum linear-stage driven by a two phase stepper motor.

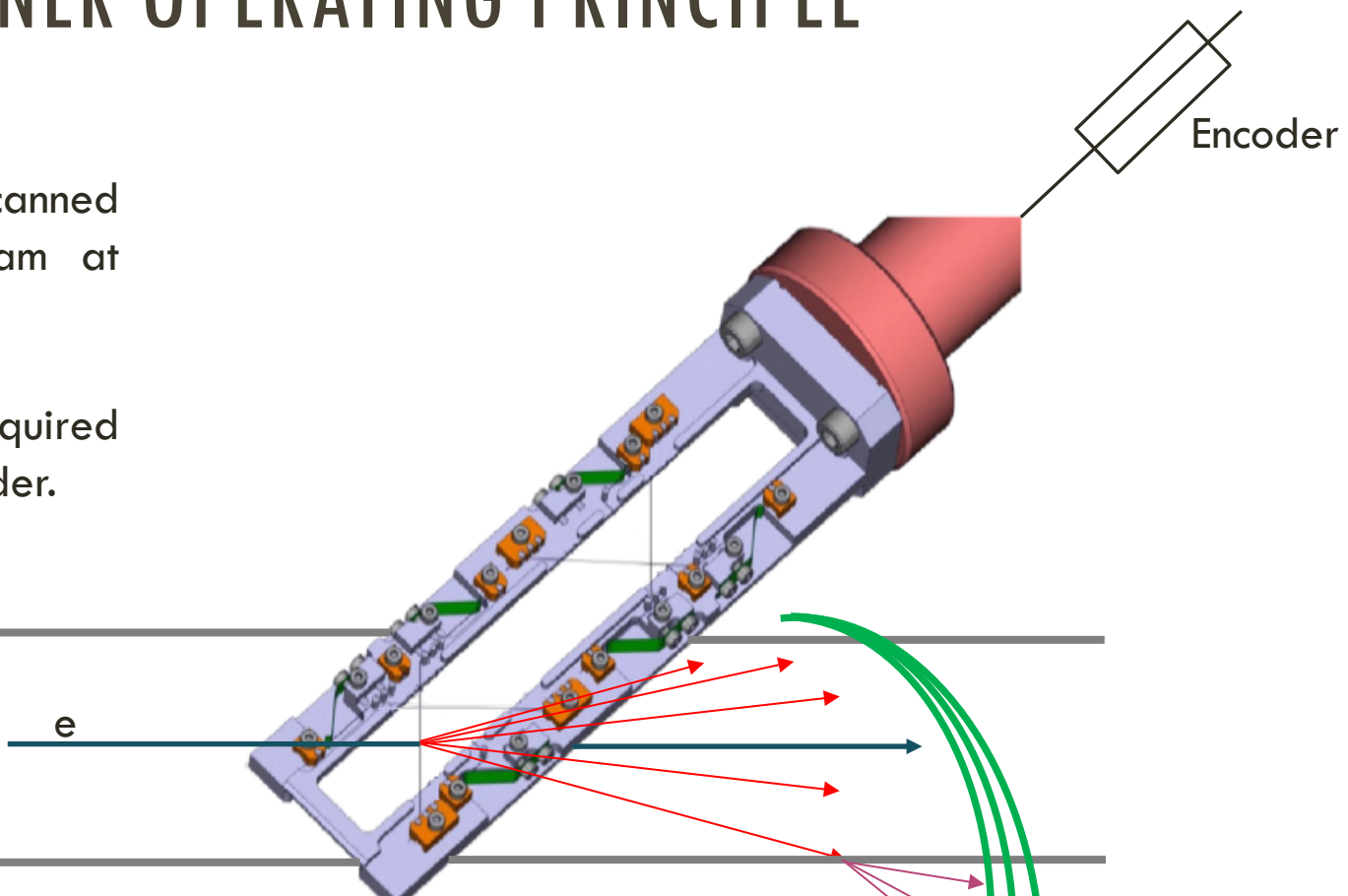
Fork inserted at  $45^\circ$  w.r.t. the vertical direction so that for each couple, one wire scans the beam vertically and the other horizontally.

# WIRE SCANNER OPERATING PRINCIPLE

A wire is scanned through the beam at constant velocity.

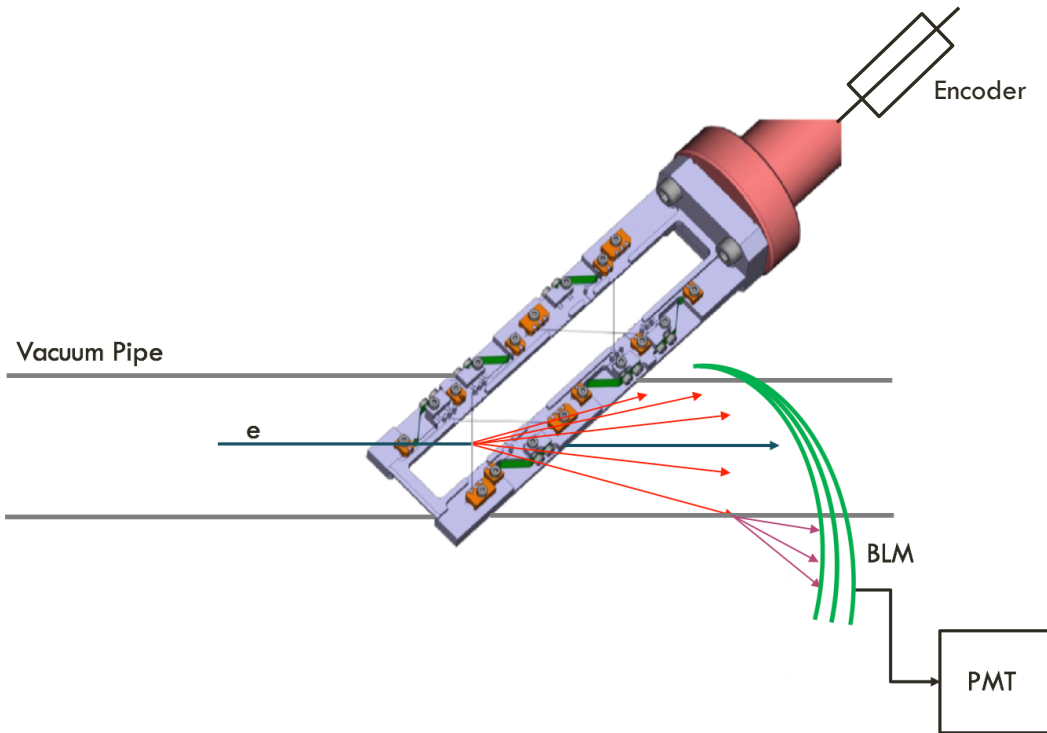
Wire position acquired by a linear encoder.

Vacuum Pipe



Shower of primary scattered electrons and secondary emitted particles ( $e^\pm, \gamma$ ) is proportional to the fraction of the beam sampled by the wire.

# WIRE SCANNER OPERATING PRINCIPLE

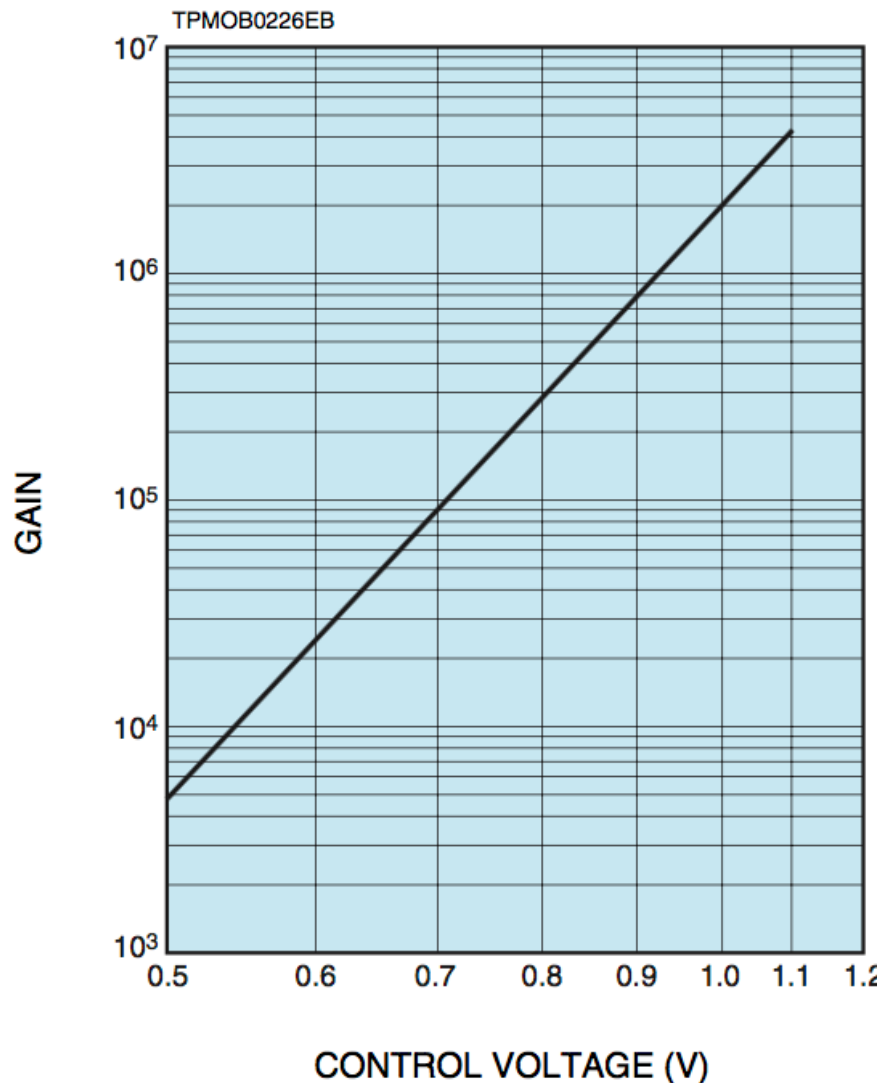


Out-of-vacuum detection of the shower's forward component through scintillator fiber.

Scintillator light sent to a PMT with an adjustable gain in the range  $[5 * 10^3, 4 * 10^6]$ .

The beam's horizontal / vertical profile can be reconstructed acquiring in beam synchronous way the wire position and BLM signal.

# BLM GAIN CURVE



# SUB-MICROMETER RESOLUTION WIRE SCANNER

## WIRE HEATING BY E-BEAM EXPOSURE

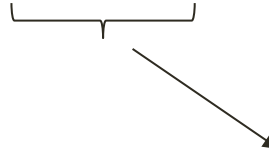
Rough estimation

**Energy transferred  
by the beam  
particles to the  
wire material**

$$E_{loss} = \frac{dE}{dt} * t * \rho_{Au} * N_e * R$$

Collisional stopping power in  
Au for  $E = 320$  MeV

$$\frac{dE}{dt} = 1.5 \text{ MeV cm}^2/\text{g}$$

  
 $N_e$    
N° of particles  
intercepted by the wire

$$R = \frac{w}{\sqrt{12}} * \frac{1}{\sigma_b}$$

$$E_{loss} = 9.6 * 10^{-11} \text{ J}$$

# SUB-MICROMETER RESOLUTION WIRE SCANNER

## WIRE HEATING BY E-BEAM EXPOSURE

Rough estimation

**Increase of  
temperature**

For each RF-shot

$$\Delta T = \frac{E_{loss}}{c_s * m_{eff}}$$

Gold specific heat

Wire effective mass

$$m_{eff} = \rho_{Au} * \sigma_b * t * \frac{W}{\sqrt{12}}$$

$$\Delta T = 3.8 \text{ K}$$

**N.B.** The computation not include any heat dissipation effect

# SUB-MICROMETER RESOLUTION WIRE SCANNER

WIRE HEATING BY E-BEAM EXPOSURE  
12.5  $\mu\text{m}$  Al & 5  $\mu\text{m}$  W wires comparison

Rough estimation

	$\Delta T$ ( °C )	Melting Point ( °C )
GOLD	3.7	1064
ALUMINUM	0.7	660
TUNGSTEN	3.7	3695

# SUB-MICROMETER RESOLUTION WIRE SCANNER

## WIRE HEATING BY E-BEAM EXPOSURE

EGS simulation

$$Q = 1 \text{ fC}$$

Energy into the wire  
for  $E_e = 350 \text{ MeV}$

$$E_{in} = 2.19 * 10^{10} \text{ keV}$$

Energy emitted as  
secondary particles

$$E_{out} = E_e + E_\gamma + E_{e+}$$

Fraction of energy  
deposited in the wire

$$Loss = \frac{E_{in} - E_{out}}{E_{in}}$$

$$Loss = 0.0015$$

$$E_{loss} = 0.525 \text{ MeV} \text{ for single } e \text{ of } 1 \text{ fC}$$

# BACKGROUND FROM THE MEMBRANE

## Beam Parameters

$E_e$	=	320 MeV
$Q_b$	=	1 pC
$\sigma_{x/y}$	=	3.2 $\mu\text{m}$

## Wire & membrane parameters

Wire Width	$w_{Au} = 2 \mu\text{m}$
Wire Thickness	$t_{Au} = 2 \mu\text{m}$
Membrane Thickness	$t_{Si_3N_4} = 0.250 \mu\text{m}$

**Radiative energy loss of the beam intercepted by the wire in the  $Si_3N_4 + Au$  thickness**

$$\Delta E \Big|_{rad}^{Si_3N_4 + Au} = \frac{E_e}{L_R^{Si_3N_4 + Au}} * t_{Si_3N_4 + Au} * \Delta N_e$$

$\downarrow$

$Si_3N_4 + Au$   
radiation length  
 $L_R^{Si_3N_4 + Au} = 0.3 \text{ cm}$

$\downarrow$

Fraction of  $e^-$  intercepted by the wire.

# BACKGROUND FROM THE MEMBRANE

**Radiative energy loss of remaining part of the beam in  $\text{Si}_3\text{N}_4$  thickness**

$$\Delta E|_{rad}^{Si_3N_4} = \frac{E_e}{L_R^{Si_3N_4}} * t_{Si_3N_4} * (N_e - \Delta N_e)$$

$\downarrow$                                      $\downarrow$

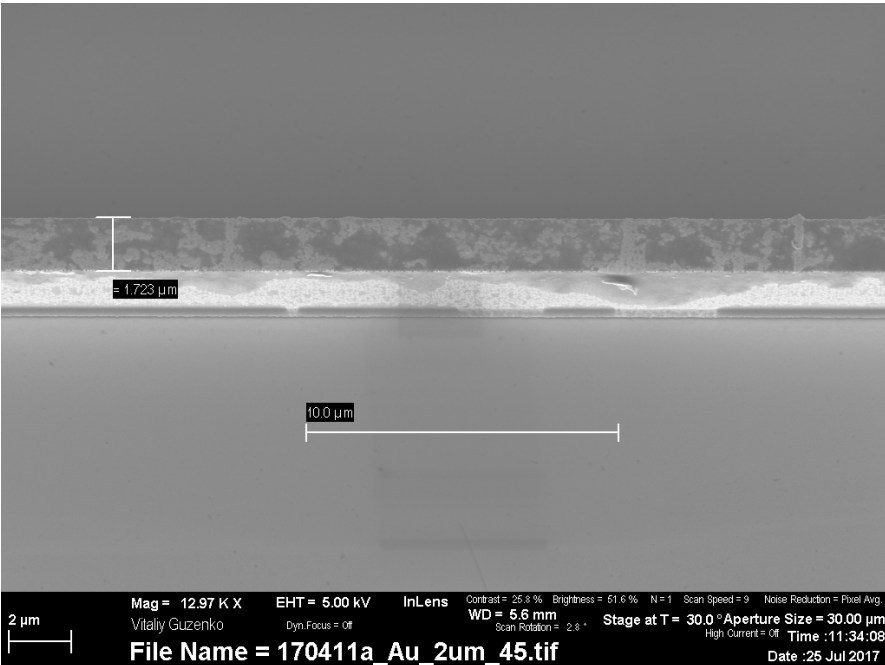
$\text{Si}_3\text{N}_4$   
radiation length  
 $L_R^{Si_3N_4+Au} = 8.3 \text{ cm}$

Fraction of  $e^-$  passing only the membrane

**Background to signal ratio**

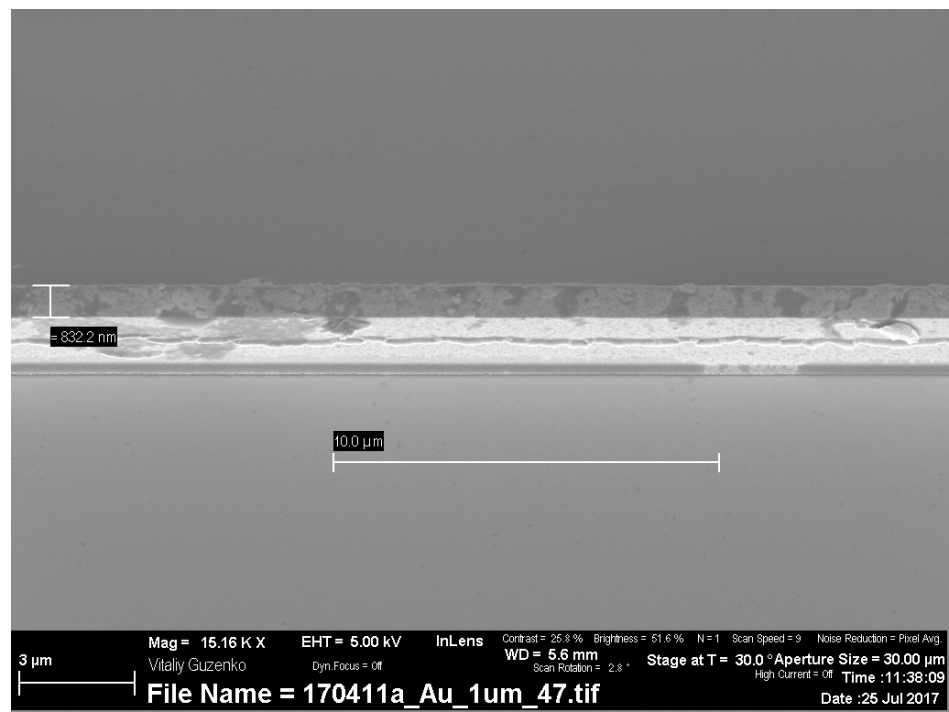
$$\frac{\Delta E|_{rad}^{Si_3N_4}}{\Delta E|_{rad}^{Si_3N_4+Au}} = 18$$

# WIRES AFTER THE BEAM EXPOSURE



**2  $\mu\text{m}$  Au wire**

$$\sigma_w = 0.6 \mu\text{m}$$



**1  $\mu\text{m}$  Au wire**

$$\sigma_w = 0.3 \mu\text{m}$$

# BEAM JITTER

From the 100 YAG screen images

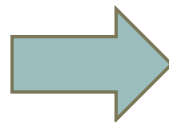
Jitter rms = 0.57  $\mu\text{m}$

Rms of the gauss fit centroids from  
the 100 YAG screen images.

# NICKEL WIRES

## Beam losses estimation

Beam loss  $\propto Z^2$



$$\frac{Au}{Ni} = 8$$

8 times  
lower signal

## Background from the membrane

Background to  
signal ratio

$$\frac{\Delta E|_{rad}^{Si_3N_4}}{\Delta E|_{rad}^{Si_3N_4+Ni}} = 9$$

# SKETCHES

# ACHIP EXPERIMENT

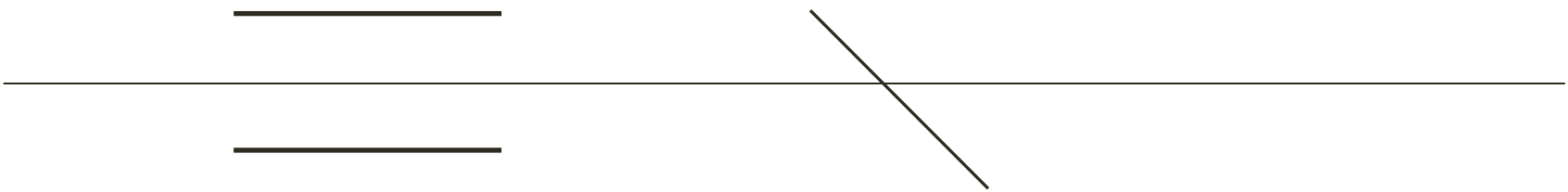
One aspect of DLAs that is significantly different from radiofrequency (rf) accelerator structures is that the transverse aperture of the accelerating structure is on the order of  $\sim 1 \mu\text{m}$

Various geometry optimizations of accelerating structures have been experimentally demonstrated  
PHOTONIC BANDGAP structures

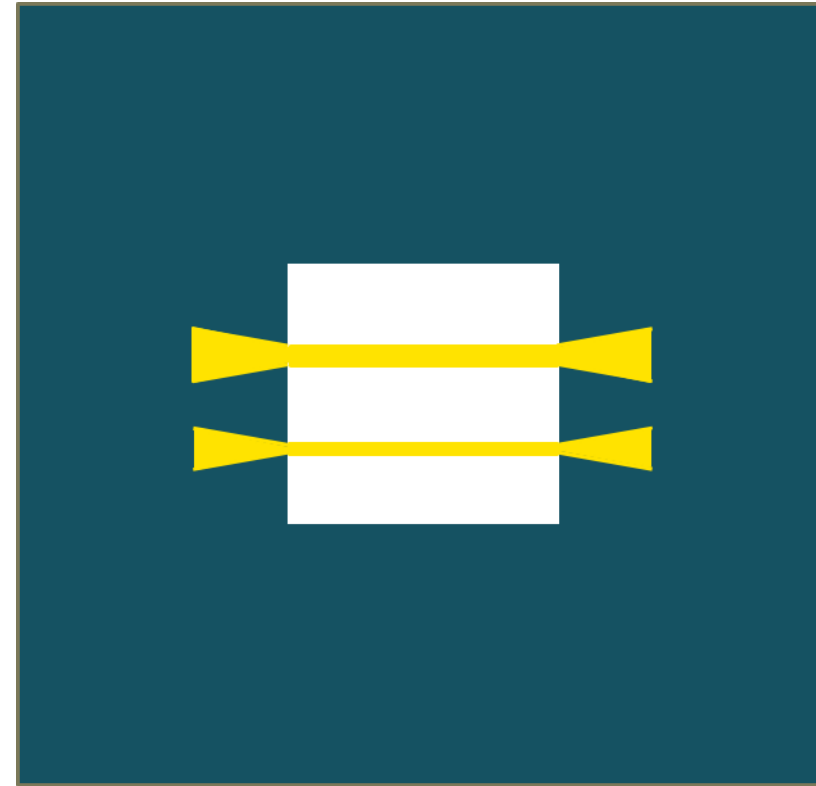
Dielectric Laser Accelerators (DLAs) are electron linear accelerators composed of dielectric microstructures powered by pulsed infrared lasers

In the case of the planar grating structure and even in more general terms, DLAs operate via laser-induced excitation of an electromagnetic field mode with a nonzero electric component parallel to the velocity of electrons traversing the mode .. the phase velocity of the excited mode must match the electron velocity.

1



# SUB-MICROMETER RESOLUTION WIRE SCANNER



# SwissFEL

Key parameters and features of SwissFEL	
Overall length (incl. experimental hall)	720 m
Total electrical power consumption	5.2 MW
Maximum electron beam energy	5.8 GeV
Height of beamline above tunnel floor	1.2 m
Electron gun	3 GHz RF gun with 2.5 cells
Cathode type	Cu photocathode driven by a frequency-tripled TiSa laser
Injector booster	Normal-conducting travelling wave structures (copper) with f=3 GHz
RF source main linac	Klystron with solid-state modulator and RF pulse compression
Accelerating structures, main linac	Normal conducting travelling wave structures (copper) with f=5.7 GHz and G=26 -28 MV/m
Linac repetition rate	100 Hz
Bunch compression	Two 4-magnet chicane bunch compressors at 0.35 GeV and 2.0 GeV, with X-band harmonic cavity at 1st bunch compressor
Number of FEL lines	2 (Aramis and Athos)
Undulator type, Aramis	In-vacuum permanent magnet with period =15 mm
Wavelength range, Aramis FEL	1Å-7Å (SASE)
Polarization, Aramis	Linear
Undulator type, Athos	Apple II permanent magnet with period=40 mm
Wavelength range, Athos FEL	7Å-70Å; seeded and SASE
Polarization, Athos	Variable (circular, elliptical and linear)

# SwissFEL

Design parameters		
Design parameters for the electron beam	Operation Mode	
	Long Pulses	Short Pulses
Charge per bunch (pC)	200	10
Core slice emittance (mm.mrad)	0.43	0.18
Projected emittance (mm.mrad)	0.65	0.25
Slice energy spread (keV, rms )	350	250
Relative energy spread (%)	0.006	0.004
Peak current at undulator (kA)	2.7	0.7
Bunch length (fs, rms)	25	6
Bunch compression factor	125	240

Performance of Aramis		
Performance of Aramis for 5.8 GeV electron energy and 1Å lasing wavelength	Long Pulses	short Pulses
Maximum saturation length (m)	47	50
Saturation pulse energy (μJ)	150(*)	3
Effective saturation power (GW)	2.8	0.6
Photon pulse length at 1 Å (fs, rms)	21	2.1
Number of photons at 1 Å (×10e9)	73	1.7
Bandwidth, rms (%)	0.05	0.04
Peak brightness (# photons.mm-2.mrad-2.s-1/0.1% bandwidth)	7.e32	1.e32
Average Brightness (# photons.mm-2.mrad-2.s-1/0.1% bandwidth)	2.3e21	5.7e18

# SwissFEL

Performance of Athos (SASE)	
Performance of Athos (SASE), for example at 3.4 GeV electron energy and 2.8 nm lasing wavelength	Long Pulses
Maximum saturation length (m)	22 m
Saturation pulse energy ( $\mu$ J)	360
Effective saturation power (GW)	11.2
Photon pulse length at 2.8 nm (fs, rms)	13
Number of photons at 2.8 nm ( $\times 10^{e9}$ )	5000
Bandwidth (%)	0.19
Peak brightness (# photons.mm <sup>-2</sup> .mrad <sup>-2</sup> .s <sup>-1</sup> /0.1% bandwidth)	6.e35
Average Brightness (# photons.mm <sup>-2</sup> .mrad <sup>-2</sup> .s <sup>-1</sup> /0.1% bandwidth)	8.e23

# SCREEN MONITORS

Two types of Screen Monitors, both for electrons and photon beams:

- Scintillating crystals: observation of fluorescence in the crystal
  - ✓ YAG
  - ✓ LuAG (factor two more visible photons)
- Optical transition radiation\* screens (OTRs): observation of the optical transition radiation on a metallic surface
  - Aluminum-coated silicon mirror to generate OTR

The visible light emitted is imaged onto area detectors like CCD or CMOOS sensors.

Due to their interceptive nature, the screens will not be inserted during routine operation.

Resolution limit:

- Finite thickness of the scintillator (seen under an angle of  $45^\circ$ )
- Angular distribution of the OTR light

\* radiation emitted when charged particles with relativistic velocities pass a metallic foil.

# GAUSS FIT

Gaussian fit to Beam Profile in the vertical as well in the horizontal plane.

## Fitting function

$$y = off + A e^{-\frac{(x-c)^2}{2\sigma^2}}$$

→ Wire Position

→ BLM loss signal

## Initial guess for the fitting parameters

Offset:

Amplitude:

Centroid:

Sigma:

off = background signal mean value

A = BLM signal – off

c = wire position value

corresponding to the BLM  
signal maximum

$\sigma$  = Integrated signal/ $A\sqrt{2\pi}$

Measure of the beam dimension

